Energy and exergy evaluation in a densified biomass burner using cocoa shells, intended for air heating for the artificial drying of food

N. Y. Castillo-Leon^{1*}, A. D. Rincon-Quintero^{1,2,3}, A. A. Mosquera-Clavijo¹, C. A. Suarez-Lopez¹, L. A. Betancur-Arboleda¹, Luis del Portillo-Valdes²

- ¹ Unidades Tecnológicas de Santander, Bucaramanga, Colombia
- ² Universidad del País Vasco UPV/EHU, Bizkaia, Spain

*Corresponding author E-mail: ncastillo@correo.uts.edu.co

Received Oct. 1, 2024 Revised Nov. 15, 2024 Accepted Nov. 26, 2024

Abstract

Residual biomass as a renewable resource provides alternatives for energy generation, turning a problem into an opportunity for the industry. This study aims to analyze the energy and exergy performance of a biomass burner that uses cocoa shells as fuel for air heating and subsequent artificial drying of food. The study involves a conventional exergy analysis evaluating the energy performance of the equipment and proposing improvements to enhance the thermal efficiency of the system. The research consists of six phases: it begins with defining the input data of the system, followed by determining the thermodynamic properties of the working fluid (air), the exergies of the biofuel and the working fluid are calculated, energy and exergy balances are performed in the heat exchanger of the burner, and efficiencies are obtained. Finally, a sensitivity analysis is conducted to understand the burner's behavior under different scenarios. The results showed an average exergy efficiency of 9.8%. By increasing energy efficiency in the sensitivity analysis, the outlet temperature rises to 164°C; however, exergy destruction decreases by 48.7%. One of the significant conclusions of this study proposes modifying the coil design to improve the exergy efficiency of the system due to its heat transfer capacity to the air.

© The Author 2024. Published by ARDA.

Keywords: Exergy analysis, Exergetic efficiency, Biofuel, Biomass burner, Artificial drying, Cocoa

1. Introduction

The utilization of biomass as a renewable energy source has gained significance due to the increasing need for sustainable alternatives to fossil fuels. Biomass, which includes agricultural residues, forestry by-products, and organic waste, offers a promising solution for the food drying process. For instance, cacao is a food that requires fermentation and drying to preserve its nutrients. Given the growing global demand and consumption, estimated at 4.824 million tons per year, Côte d'Ivoire and Ghana are the leading producers, accounting for 63% of the global market, while Colombia ranks tenth with a production share of 1.2%. However, the International Cocoa



³ Sistema General de Regalías SGR, Ministerio de Ciencia Tecnología e Innovación, Colombia

Organization (ICCO) recognizes that 95% of Colombian cacao possesses characteristics that distinguish it for its fine flavor and aroma, creating a competitive advantage for the Colombian cocoa sector, as only 5% of the total cacao produced globally has these organoleptic attributes [1,2].

To address the challenges associated with biomass combustion and optimize its use, various techniques have been developed that are adapted to the characteristics of biomass, such as direct combustion, gasification, and pyrolysis. In particular, for artificial food drying processes, direct combustion technology allows for the utilization of biomass energy and its transfer in the form of heat to the working fluid, which subsequently performs the drying of the product.

Despite advances, the developed methods present disadvantages, the main one being the lower heating value of biomass, which ranges from approximately 11 to 15 MJ/kg, compared to conventional fossil fuels that approach 43.50 MJ/kg. This results in low energy and exergy efficiencies of 10.62% and 9.4%, respectively, with exergy destruction of 82% in the system, indicating a significant loss of useful energy [3, 4, 5].

Burners are characterized as devices that utilize direct combustion of biomass, generating an exothermic chemical reaction between oxygen and fuel, which is then transferred as heat to the working fluid (air). The thermal performance of a biomass burner can be assessed through calculations based on the first and second laws of thermodynamics, providing data on the energy efficiency of the equipment, losses due to irreversibility, and thus enabling design optimization [6].

The first law presents a mass and energy analysis through heat exchange between systems. This approach allows for the calculation of thermal efficiency, a key indicator for determining functionality and the amount of energy utilized in the process. However, the limitation of this law is that it does not account for all endogenous and exogenous energy losses involved in the system. Therefore, studies based on the second law of thermodynamics are conducted, establishing that in any transfer or conversion of energy within a closed system, entropy increases. This term defines the inequalities based on the reversibility of a system [3,6].

For this reason, the exergy analysis is conducted to quantify the irreversibility of the studied technology, such as heat transfer losses within the system and the process in relation to its environment [6,7,8]. Therefore, it is necessary to identify the components with the highest exergy destruction and loss, along with the processes that cause them. Improving the overall efficiency of the burner can be achieved by reducing exergy destruction in the various equipment of the process, even though certain irreversibilities are inevitable [9,10]. Table 1 presents experimental research related to the energy and exergy evaluation of combustion systems.

Table 1. Studies related to the energy and exergy evaluation of combustion systems

Author	Raw Material	Final Application	System Type	Key Results
[10]	Biomass	Multigeneration System	Steam Turbine	Energy Efficiency=20,2 % Exergy Efficiency= 15,2 %
[8]	Sulfuric Acid	Energy Losses	Steam Plant	Key sources of exergy destruction: Waste Heat Boiler= 41%, Heaters = 24,7% Steam Turbine= 18,6% Condenser = 13,8%
[11]	Kerosene Wax	Trigeneration (electricity, heating, and cooling)	Organic Rankine Cycle (ORC)	Maximum exergy efficiency of ORC = 13%, when trigeneration is used = 28%. The biomass burner contributes 55% of the total destroyed exergy, while the

Author	Raw Material	Final Application	System Type	Key Results		
				ORC evaporator contributes 38% of the total destroyed exergy.		
		Chemical		Exergy destruction percentages:		
[7]	Cellulose and	Recovery of	Coconomotion	RB=41,63		
[7]	Paper	Black Liquor and	Cogeneration	PB =33,5%		
		Soda		Maximum exergy efficiency= 32,09%		
			Exergy efficiency of the refrigerator with distiller			
	Refrigerator	Improve exergy efficiency and	Absorption	η ex = 24,37% at 86 °C		
[9]				Total exergy loss		
		minimize exergy losses	Refrigerator	Ex1, tot = $457,45 \text{ kW}$		
		103363		Refrigerator with rectifier		
				η ex = 22,34% at 85 °		
[12]	Air	Structural Improvement	Boiler	Exergy efficiency of the boiler increased from 47,29% to 48,35%		
[13]	Ammonia	Decarbonization of Maritime Transport	Fuel Cell	Exergy efficiency = 61,10%, Exergy efficiency of SRC = 41,21%		

Considering the reviewed literature, studies evaluating different methodologies for calculating energy and exergy efficiencies were found. However, most studies focus on specific boiler systems that use biomass as fuel, highlighting a lack of research related to combustion systems for food drying [10,11,12]. Based on this, the objective of this study is to develop a conventional exergy analysis of a biomass burner device intended for air heating for the artificial drying of cacao. The process combusts pellets made from cacao shells and transfers thermal energy to a heat exchanger, which is flooded with motor oil, stabilizing the temperature of the air passing through the coil.

This study is conducted from an analytical approach, examining the formulations and assumptions involved in the process, allowing for the evaluation of thermodynamic performances in different scenarios through sensitivity analysis, varying the thermal efficiency, lower heating value, and mass flow rate of air.

The structure of this research is presented as follows: the configuration and experimental tests conducted on the biomass burner (case study) are described to identify the thermodynamic variables affecting the air heating process. Hourly data obtained are averaged to carry out mass, energy, and exergy balances, as well as a direct uncertainty analysis and the proposed sensitivity for the case study. Subsequently, a study of the results is presented, along with a discussion of the work performed, evaluating the thermal performance of the equipment, and finally, the conclusions of the research are outlined.

2. Research method

2.1. Description of the experimental setup

2.1.1. System description

An experimental setup is proposed for air heating using a biomass burner. The main components are illustrated in Figure 1, which includes: (1) ambient temperature air inlet to the coil, (2) hot air outlet from the coil, (3) heat exchanger, (4) casing or body of the burner, (5) biomass combustion chamber, and (6) ash collection.

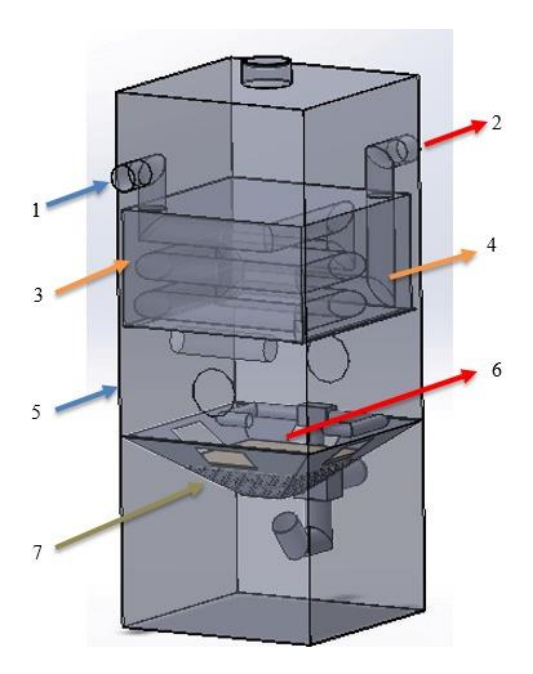


Figure 1. Schematic view of the experimental setup under study

Figure 2 shows a photograph of the biomass burner setup analyzed at the study site. Its design includes a 16-meter-long stainless steel duct coiled in the shape of a spiral, which is submerged in motor oil, acting as a heat exchanger. The inlet and outlet of the pipe are located outside the casing, with connections to the compressor and the drying chamber, respectively. The equipment has an ignition chamber where the combustion process of the biomass takes place, releasing energy in the form of heat, which is transferred to the oil container and finally to the fluid (air) circulating through the steel coil.



Figure 2. Photograph of the experimental setup

2.1.2. Technical specifications

Table 2 illustrates the technical characteristics of the system, detailing each of its components. The main element of the densified biomass burner is the stainless steel coil, which has a diameter of 3/4 inches and a length of 16 meters. All of this is submerged in a 12-liter tank of motor oil, which serves as a thermal stabilizer. The stainless steel combustion chamber has a capacity of 16 kg of biomass (pellets) for a 16-hour drying cycle.

Table 2. Technical specifications of the system							
	Air Coil						
Specification	Value	Units					
Material	Stainless Steel	-					
Diameter	3/4	in					
Gauge	18	-					
Length	16	m					
Working Fluid	Air	-					
	Storage Tank and Heat Exchanger						
Specification	Value	Units					
Material	Stainless Steel	-					
Width, Length, Height	38x38x22	cm					
Stabilization Fluid	Motor Oil	-					
Capacity	12	L					
C	Combustion Chamber and Fuel Basket						
Specification	Value	Units					
Material	Stainless Steel	-					
Capacity	1	kg/h					

Table 2. Technical specifications of the system

2.1.3. Error propagation

In the experimental trials aimed at evaluating temperatures, pressures, and velocities in the pellet burner, the occurrence of errors and uncertainties related to the selection and calibration of instruments, data reading, approximations, and test preparation is likely. For this reason, this study applies the statistical technique of error propagation, which helps improve measurement accuracy [13]. Initially, the following equation is considered, indicating the average of the experimentally obtained data for each thermodynamic variable, defined as an average function of the individual factors provided. $\bar{x}x_i$.

$$\bar{x} = \frac{\sum_{i=1}^{n} (x_i)}{n} \tag{1}$$

Subsequently, Equation 2 is used to calculate the standard deviation of the experimental measurements with respect to the mean.

$$\sigma = \left(\frac{\sum (x_i - \bar{x})^2}{(n-1)}\right)^{\frac{1}{2}} \tag{2}$$

Finally, Equation 3 is used to evaluate the relative uncertainty regarding the pressures, temperatures, and velocities obtained during the tests.

$$\delta = \frac{\sigma}{\bar{x}} = \left(\frac{1}{n} \sum_{i=1}^{n} \frac{(x_i - \bar{x})^2}{(n-1)}\right)^{\frac{1}{2}}$$
(3)

The direct uncertainties during the measurements of the thermodynamic parameters in the biomass burner are presented, as detailed in Table 3. This table includes the references and precisions of the instruments used for data collection, which are essential for analyzing the performance of the biomass burner. Figure 3 illustrates the measuring equipment, which includes an anemometer to measure inlet and outlet velocities and a DHTT-22 sensor to monitor the temperatures of the working fluid. It is important to note that the pressure drop was determined using analytical methods, as the obtained values are below the measurement range of the instrument used.

TD 11 0	D 1		1 .	.1 .	C	
Table 3	Relative	uncertainty	during	the measurement	Ωŧ	narameters
Table 5.	1Clatt v C	unccitainty	uuring	tiic iiicasaiciiiciit	OI	parameters

		•			
Parameter	Unit	Measurement Sensor	Reference	Accuracy	Uncertainty
Exit air velocity	[EM]	Anemometer (Figure 3A)	GM-8901, China	±2%	±0.052
System temperature	[°C]	Sensor (Figure 3B)	DHT-22	±1,5 °C	$\pm 0,188$

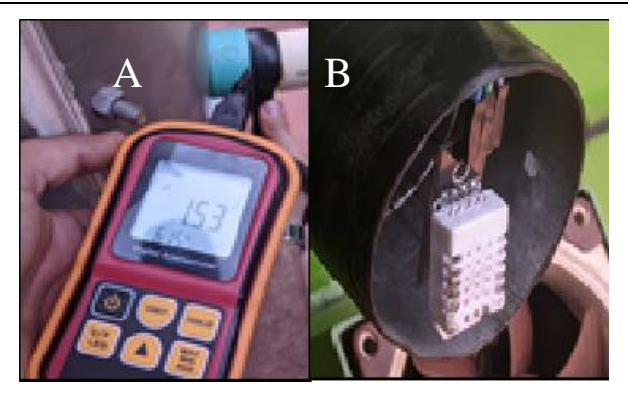


Figure 3. a) Speedometer b) Temperature sensor

2.2. Conducting the experimental tests

To initiate the tests, it is verified that the burner meets the following conditions: the collection tray must be free of ashes, and the perforations in the base of the combustion chamber and the ventilation openings must be unobstructed; the automated screw conveyor system for the addition of the biofuel must be functioning correctly, adhering to the activation cycle times; the measurement and sensing instruments must be properly calibrated to avoid obtaining data with a significant margin of error; the biofuel used must be completely free of moisture; otherwise, the burner will operate below its designed performance. Figure 4 shows the path of the working fluid acquiring thermal energy through the combustion of biomass.

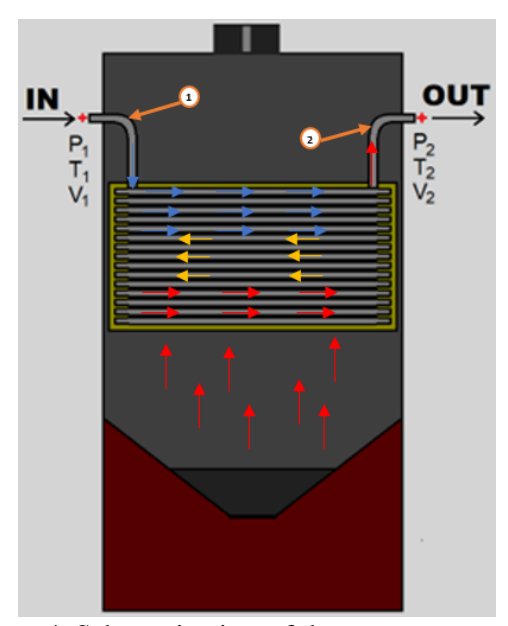


Figure 4. Schematic view of the system test points

The experimental tests were conducted over 16 hours, divided into two days, starting at 2:00 PM and ending at 10:00 PM, with data collection intervals every 2 hours. These data were recorded using measurement instruments, obtaining values for temperatures, velocities, and pressure within the system, which are the variables influencing the air heating process inside the burner.

3. Results and discussion

3.1. System analysis

The phases for conducting the energy, exergy, and sensitivity analysis of the studied biomass burner are divided into three steps: the first phase involves determining the initial parameters of the system, which are shown in Table 4; then, the formulation of the proposed analyses in the research; and finally, the consideration of the performance of the studied equipment.

Operating at an ambient temperature of 25 °C, the system reaches a combustion temperature of 577.35 °C, while the oil is maintained at 67 °C. The measured air volume is 0.78 m³/kg, where the theoretical chemical exergy of the air is calculated at 34.05 J/mol, taking into account the ideal gas constant of 8.314472 J/mol*K and a specific heat capacity of air of 1.007 J/kg*K. The energy characteristic of the biomass is given by the lower heating value of cocoa shell pellets, which for this study is 11.7 MJ/kg [14], ensuring efficient performance in the system, and allowing for continuous operation over 16 hours.

Table 4. Initial parameters of the system						
Parameter	Value	Units	Reference			
Ambient temperature	25	°C	[15]			
Combustion temperature	577,35	$^{\circ}\mathrm{C}$	[16]			
Oil temperature	67	°C	[17]			
Ambient pressure	101,325	kPa	[18]			
Specific volume of air	0,78	m ³ /kg	[19]			
Theoretical chemical exergy of air	34,05	J/mol	[20]			
Ideal gas constant	8,314472	J/mol*K	[21]			
Specific heat of air	1,007	J/kg*K	[22]			
Molar mass of air	28,7364	kg/mol	[23]			
Lower heating value of biofuel (cocoa shell)	11,7	MJ/kg	-			
Operating time	16	h	[24]			

Table 4. Initial parameters of the system

3.2. Exergy composition of cocoa shell

The cocoa shell has an exergy value, which refers to the amount of useful energy that can be obtained from this biofuel [9]. The exergy flow in a system consists of chemical and physical exergy. The chemical exergy indicates the energy produced by the chemical reactions of its components, while the physical exergy applies to systems influenced by kinetic energy; therefore, in this study, physical exergy is considered negligible.

To calculate the chemical exergy of the densified cocoa shell biomass (pellet), the chemical compositions of the biofuel were used. The beta and the chemical exergy of the cocoa shell (Table 5) were determined using Equations 14 and 13, respectively [25].

Table 5. The chemical exergy contained in the cocoa shell

Parameter	Units	Value
Beta β	-	1,130
Chemical exergy of cocoa shell	kJ/kg	13.248,38

The chemical exergy of the cocoa shell, as seen in the previous table, has a value higher than that of its lower heating value. The reason for this is that exergy accounts for the entire useful potential of the biofuel. The difference between the two is approximately 2,000 kJ/kg.

3.3. Energy and exergy formulation

To determine the values of the system variables—temperature (T), pressure (P), and velocity (V)—measured at the inlet and outlet of the equipment, and to conduct the energy and exergy analysis, formulas are used to

calculate these magnitudes. This is done using a thermodynamic state computation tool (CoolProp) through the Helmholtz energy equations [15,16, 25].

Once the thermodynamic properties of each point have been obtained, the following can be calculated:

• Input energy to the system provided by combustion

$$E_{in} = LHV_{cocoa} * m_{cocoa} * t (7)$$

Where PCI is the lower heating value of the cocoa shell and t is the operating time of the burner.

• Heat transferred to the airflow in the heat exchanger

$$\dot{Q}_{air} = \dot{m}_{air} * Cp_{air} * (T_{out} - T_{in})$$
(8)

Exergy flow per unit mass

$$e_x = e_{physics} + e_{chemistry} \tag{9}$$

The exergy flow is also expressed as the product of exergy per unit mass and the mass flow rate.

$$Ex = e_x * \dot{m} \tag{10}$$

To determine the physical and chemical energies of the air, the following two equations are used.

$$e_{ch.air} = \frac{\bar{e}_{ch.air} + R * T_o * ln\left(\frac{P_o}{P_i}\right)}{\sum X_i * Y_i}$$
(11)

$$e_{ph.air} = (h_i - h_o) + T_o * (s_i - s_o)$$
(12)

• Chemical exergy of the cocoa shell per unit mass

$$e_{ch-cocoa} = (LHV_{cocoa}.\beta) + (bchs - Cs).zs + bcha.za + bchw.zw$$
 (13)

Where, bcha corresponds to the chemical exergy of the ash, although it is usually disregarded, bchs is the chemical exergy of sulfur, and bchw is the chemical exergy of water; zs, za y zw refer to the mass fractions of sulfur, ash, and water, respectively. The expression (bchs - Cs) was determined based on standard values described in the book; Exergy analysis of thermal, chemical, and metallurgical processes [26, 27].

$$\beta = \frac{1.044 + 0.016 \left(\frac{H}{C}\right) - 0.3493 \left(\frac{O}{C}\right) \left[1 + 0.0531 \left(\frac{H}{C}\right)\right] + 0.0493 \left(\frac{N}{C}\right)}{1 - 0.4124 \left(\frac{O}{C}\right)}$$
(14)

Where C, H, O, and N refer to the mass fractions of Carbon, Hydrogen, Oxygen, and Nitrogen, respectively, contained in the biofuel, specifically the cocoa shell.

• Exergy destroyed in the burner

$$\dot{E}x_{dest} = \dot{E}x_{innuts} - \dot{E}x_{products} \tag{15}$$

Thermal efficiency of the burner

$$\eta_{burner} = \frac{\dot{Q}_{air}}{\dot{Q}_{fuel}} \tag{16}$$

Where \dot{Q}_{fuel} is the heat flow provided by the cocoa shell during the combustion process.

Exergetic efficiency in the system

$$\eta_{exergetic} = \frac{\dot{Q}_{air}}{\dot{E}\dot{x}_{cocoa}} \tag{17}$$

Where $\dot{E}x_{cocoa}$ It is determined by the chemical exergy of the cocoa shell multiplied by the mass flow rate of the biofuel. It can also be determined by:

$$\eta_{exergetic} = 1 - \frac{\dot{E}_{Total,dest}}{\dot{E}x_{cocoa}} \tag{18}$$

• Exergy destroyed in the system.

$$\dot{E}x_{T,destroyed} = \dot{E}x_{dest,burner} \tag{19}$$

• Loss of exergy in the system.

$$\dot{E}x_{T,perd} = \dot{E}x_{T,in} - \dot{E}x_{T,prod} - \dot{E}x_{T,dest}$$
(20)

3.4. Methodology diagram

The methodology used for the thermodynamic analysis of the first and second laws is described in Figure 5.

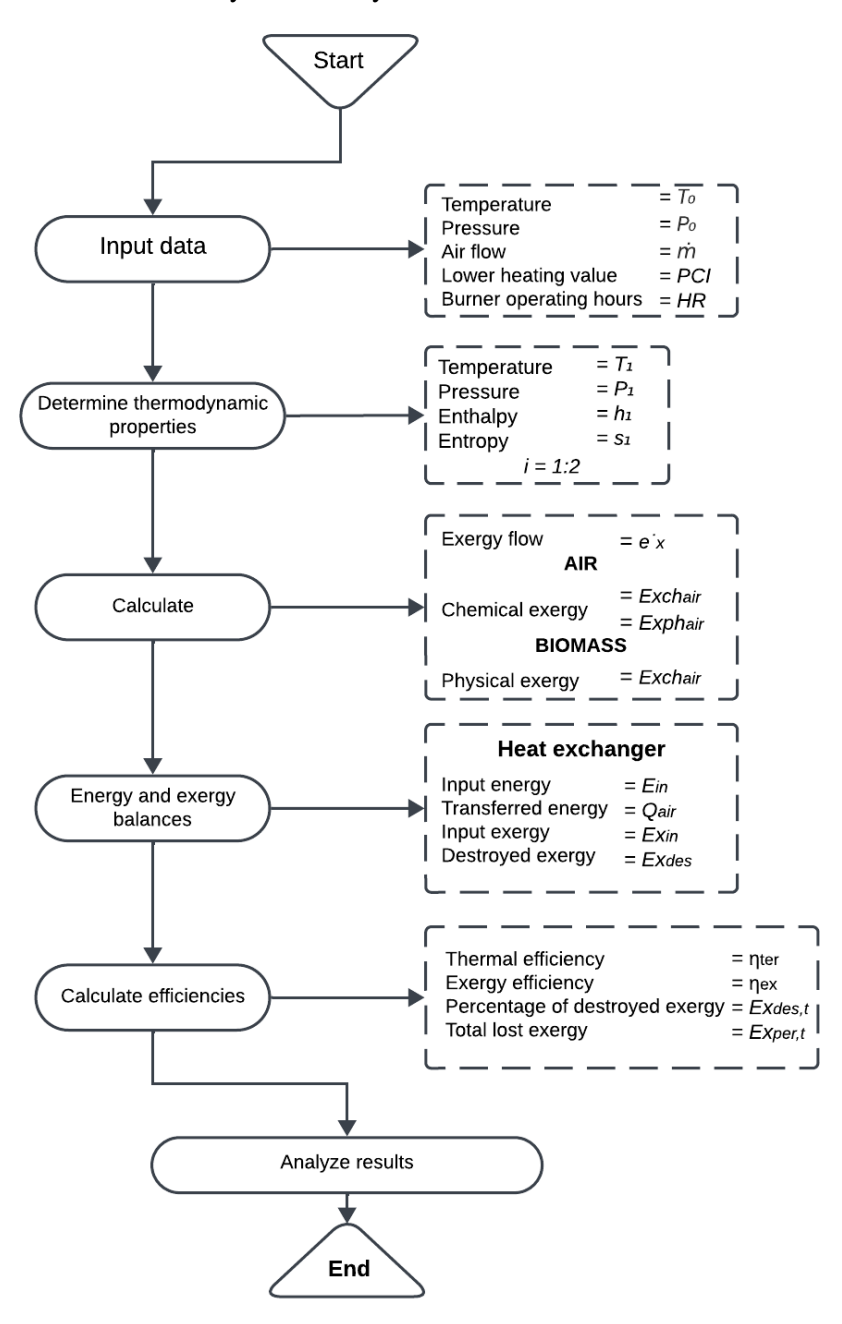


Figure 5. Diagram with the methodology of the exergetic analysis

3.5. Sensitivity analysis

The purpose of this analysis is to understand the energy performance of the system by varying the energy efficiency, the lower heating value of the fuel, and the mass flow rate of the air, projecting results for future engineering applications.

The first variable that fluctuated is the thermal efficiency at -50%, +50%, +100%, +150% and +200%. The second variable is the lower heating value (LHV), varying at -50%, +50%, +100%, +150% and +200%. Lastly, the mass flow rate of the air is varied at -50%, +50%, +100%, +150% and +200%, resulting in new outcomes for heat transfer efficiency, which reflects a lower destruction of exergy in the system.

3.6. Calculations of the thermodynamic properties of the system

Based on the methodology outlined in Figure 5, to conduct the conventional energy and exergetic analysis, it is necessary to know the physical and thermodynamic properties of the system (Table 6), determined at three points: the environment or surroundings, which will serve as the reference for the exergetic analysis, the inlet of the burner, and finally, the outlet of the burner.

Table 6. Thermodynamic properties obtained from the tests

			1 1						
	Reference environment								
Property	Units	14:00	16:00	18:00	20:00	22:00			
Temperature	K	298,15	298,15	298,15	298,15	298,15			
Pressure	Pa	101.300	101.300	101.300	101.300	101.300			
Enthalpy	J/kg	424.436,10	424.436,10	424.436,10	424.436,10	424.436,10			
Entropy	J/kg*K	3.880,56	3.880,56	3.880,56	3.880,56	3.880,56			
		I	Burner inlet						
Temperature	K	298,65	298,5	298,7	298,55	298,5			
Pressure	Pa	20.3400	198.050	197.800	197.800	197.800			
Velocity	m/s	3,185	3,185	3,185	3,185	3,185			
Enthalpy	J/kg	424.706,03	424.567,06	424.769,20	424.618,02	424.567,63			
Entropy	J/kg*K	3.681,46	3.688,64	3.689,68	3.689,17	3.689,00			
		В	Surner outlet						
Temperature	K	349,25	352,05	357,15	334,3	332,7			
Pressure	Pa	203.400	198.050	197.800	197.800	197.800			
Velocity	m/s	3,185	3,185	3,185	3,185	3,185			
Enthalpy	J/kg	475.757,21	478.594,69	483.749,28	460.670,84	459.056,04			
Entropy	J/kg*K	3.839,37	3.855,11	3.870,00	3.803,22	3.798,39			

Note: The data obtained from both days were averaged into a single table.

It is necessary to determine the mass flow rate of the working fluid circulating through the burner pipe, which in this case is air. This is calculated at a single point since the equipment is considered a steady-flow system. Therefore, the mass flow rate at the inlet and outlet will be equivalent, as shown in Table 7.

Table 7. Airflow in the system

Property	Units	14:00	16:00	18:00	20:00	22:00
Density	m³/kg	2,3741	2,3128	2,3083	2,3095	2,3099
Mass flow rate	kg/s	0,0075	0,0073	0,0073	0,0073	0,0073

Note: The data obtained from both days were averaged into a single table.

3.7. Energy calculations

To determine the energy entering the system, Equation 7 was implemented. The energy transfer from combustion to the air was calculated using Equation 8, and the energy efficiency was calculated using Equation 16 compiled in Table 8.

Property	Units	14:00	16:00	18:00	20:00	22:00	
Input energy	kW	3,25	3,25	3,25	3,25	3,25	
Energy transfer	kW	0,3834	0,3954	0,4308	0,2636	0,2522	
Energy efficiency	%	11,80	12,17	13,26	8,11	7,76	

Note: The data obtained from both days were averaged into a single table.

The input energy is constant and does not vary, as it comes from cocoa shell and the frequency of biomass addition to the combustion process is always maintained. The required amount is one kilogram per hour (1 kg/h), and it remained constant during both test days.

The energy transferred or heat flow from the burner was calculated using the inlet and outlet temperatures. The greater the temperature difference between these two points, the greater the magnitude of energy transfer, indicating a direct proportionality. By knowing the total input energy values and the energy transferred by the burner to the air, it is possible to determine the energy efficiency of the system. A decrease in efficiency was observed during nighttime hours.

3.8. Exergy of the working fluid

Just like fuel, air has an exergy value, divided into chemical and physical exergy. The chemical part refers to the chemical reactions occurring due to the components of the air, while the physical part is related to the mechanical properties of the element. The chemical exergy is determined in Table 9 using Equation 11. To calculate the difference in physical exergy between the inlet and outlet, Equation 12 is used.

Table 9. Exergetic parameters of air: physical and chemical

	_		1 -			
Parameter	Units	14:00	16:00	18:00	20:00	22:00
Chemical Exergy	J/kg	2.041,62	2.041,62	2.041,62	2.041,62	2.041,62
Physical Exergy (Outlet - Inlet)	J/kg	98.129,52	103.660,38	112.741,37	70.056,73	67.100,87

By observing the chemical exergy, it can be determined that there is no variation in exergy, since the air entering the system does not cause any chemical reactions, does not mix, and does not change state. This value remains unchanged, as the chemical composition at the inlet is the same as that at the outlet. The value of chemical exergy is lower than that of physical exergy. In this case, physical exergy is relevant because the air is in motion with an increase in temperature and pressure.

Physical exergy was calculated using the thermodynamic properties of air at two points: inlet and outlet. This procedure primarily requires the use of entropy; if for any reason these are omitted from the equation, the result would simply transform into an energy calculation, which is not necessary at this point in the research.

3.9. Exergy calculations

The change in exergy within the system described in Table 10 is determined by the exergy exiting the burner minus the exergy entering it. This difference is used to calculate the exergetic efficiencies; therefore, as the outlet exergy increases, the difference grows, proportionally affecting the calculation of the inputs. Table 11 presents the energetic efficiencies of the system.

Table 10. Difference in exergy between the outlet and inlet of the burner

Property	Units	14:00	16:00	18:00	20:00	22:00
Exergy Differential (Outlet - Inlet)	J/kg	98.129,52	103.660,38	112.741,37	70.056,73	67.100,87

Note: The data obtained from both days were averaged into a single table.

		8 - 1		3		
Property	Units	14:00	16:00	18:00	20:00	22:00
Inputs	kW	3,68	3,68	3,68	3,68	3,68
Outputs	kW	0,7385	0,7600	0,8251	0,5130	0,4914
Destroyed Exergy	kW	2,941	2,9200	2,8549	3,1670	3,1886
Lost Exergy	kW	0,3550	0,3646	0,3943	0,2494	0,2392
Exergetic Efficiency	%	10,42%	10,74%	11,71%	7,16%	6,85%

Table 11. Exergetic efficiencies of the system

Note: The data obtained from both days were averaged into a single table.

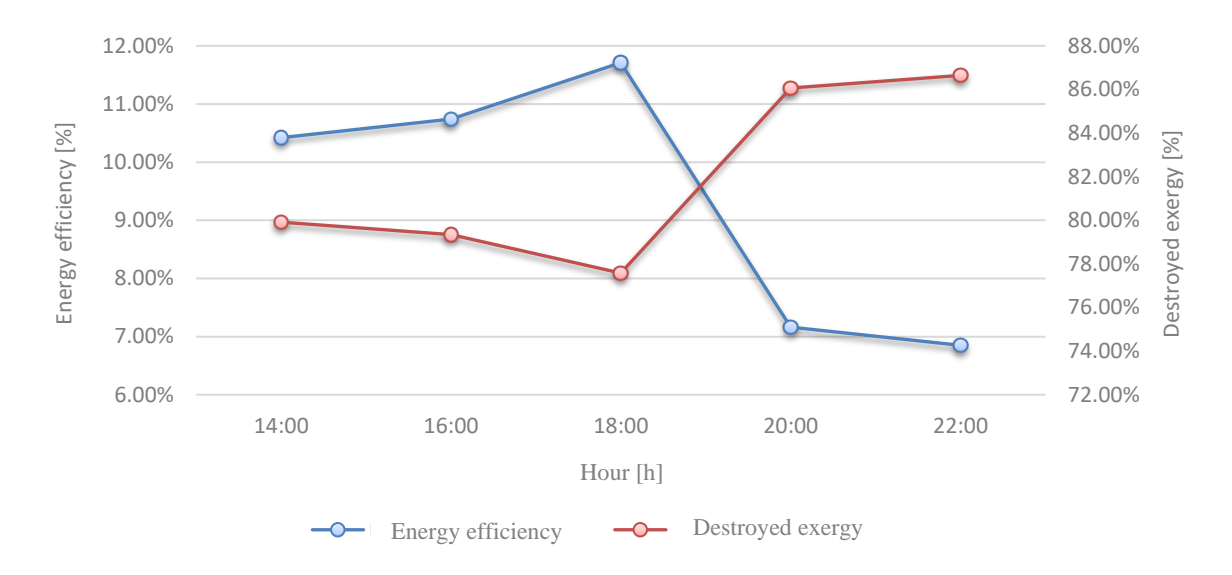


Figure 6. Graph of the thermodynamic behavior of the burner during operation

As seen in Figure 6, the percentage of destroyed exergy increases as evening approaches, which also affects the exergetic efficiency, decreasing inversely proportional to the percentage of destroyed exergy. When comparing the magnitude of the input energy with the exergetic inputs, it can be observed that the exergetic value exceeds the energetic value by approximately 480 Watts, which represents a significant figure if one wishes to consider all the energy that can theoretically be converted into useful work by the system.

The outputs represent the portion of the inputs that have been transformed into forms of energy that can be used to perform useful work, meaning that the outputs contain the energy that has not been dissipated as waste heat caused by entropy. To calculate the outputs, the exergy differential between the inlet and outlet is used, multiplied by the mass flow rate of the air.

It is important not to confuse the results of destroyed exergy and lost exergy. When referring to destroyed exergy, it denotes the energy that cannot be utilized due to irreversibilities in the system. In contrast, lost exergy consists of energy that flows to the surroundings and, therefore, cannot be used by the system.

Exergetic efficiency indicates the performance of the system, comparing the values of useful work with the total energy supplied. Calculations yield an average exergetic efficiency of 9.4%, which is relatively low and serves as an indicator used in the proposed sensitivity analysis.

3.10. Sensitivity analysis

The sensitivity analysis is developed to observe the behavior of the biomass burner by adjusting various input parameters at different percentages, starting from the current state. This allows for an optimal study of the system and helps identify critical factors that cause inefficiencies, as well as assists in establishing improvement solutions for process performance.

The results of the proposed sensitivity analysis are presented below, with the chosen variables determined due to their strong relationship with the thermal performance of the system.

3.11. Case 1: Adjustment of energy efficiency

Energy efficiency varies according to the design of the equipment, materials, and other factors that influence the optimal energy utilization of the system. For example, as shown in Table 12, constructing the equipment with materials of high thermal conductivity, phase change materials (PCM), and thermal insulation, along with geometric optimizations in the design, can significantly improve efficiency.

Table 12. Sensitivity case 1

Variation of Efficiency	-50%	Current	50%	100%	150%	200%
Energy Efficiency [%]	5,31	10,62	15,93	21,24	26,55	31,86
Outlet Temperature [°C]	48,27	71,54	94,80	118,07	141,34	164,61
Exergy Destruction [%]	90,96	82,00	73,35	64,94	56,72	48,67

Calculating the new energetic efficiencies shown in Table 10, it is analyzed in Figure 7 that as eWnergy efficiency increases, the outlet temperature rises to 164°C with an efficiency of 31.8%. On the other hand, the destruction of exergy decreases by 33 percentage points.

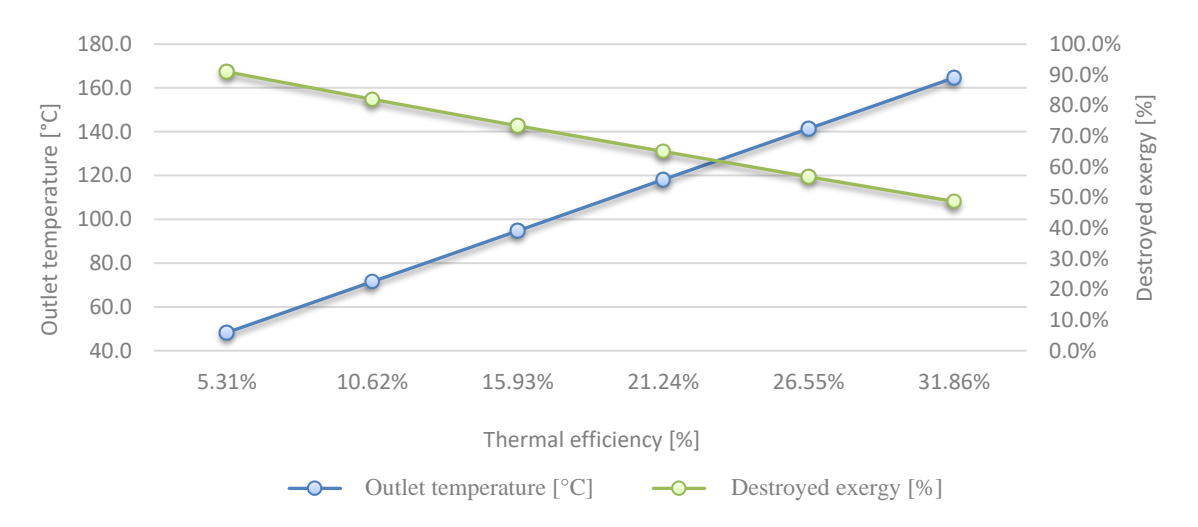


Figure 7. Sensitivity graph case 1

3.12. Case 2: Adjustment of the lower heating value (LHV)

The heating value is a property of biomass that establishes the amount of energy contained per unit of mass and varies depending on the fuel composition. Making adjustments to the lower heating value involves techniques to improve the quality of the biomass. For example, pretreatments to reduce moisture or mix with other biomass types to enhance their energy content can be employed, as outlined in Table 13.

Table 13. Data obtained from adjusting the lower heating value (LHV)

Variation of LHV	-50%	Current	50%	100%	150%	200%
Lower Heating Value [kJ/kg]]	5.850	11.700	17.550	23.400	29.250	35.100
Outlet Temperature [°C]	48,27	71,54	94,80	118,07	141,34	164,61
Exergy Destruction [%]	81,95	82,00	82,22	82,45	82,67	82,87

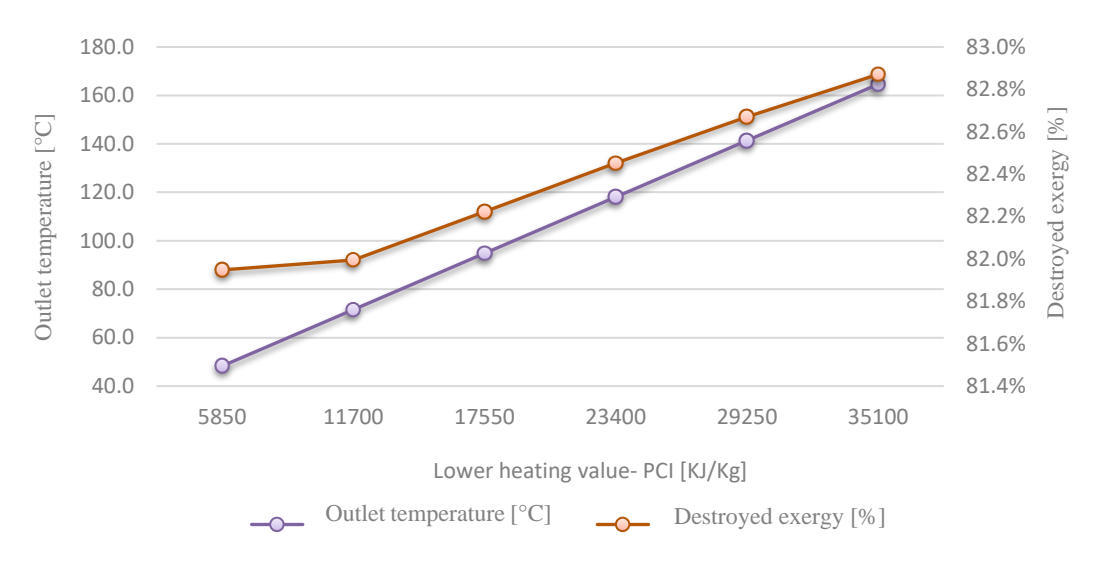


Figure 8. Sensitivity graph case 2

Figure 8 shows that as the lower heating value of the fuel increases, the outlet temperature rises to 164°C, similar to the increase observed with energy efficiency. However, it is noted that exergy destruction increases by about 1%, indicating that the energetic potential of the biomass is not being fully utilized. This is primarily because this indicator is closely tied to the energy efficiency of the equipment.

3.13. Case 3: Adjustment of the mass flow rate of air

The mass flow rate of air is the amount of kilograms of air per second flowing through the coil. The flow rate described in Table 14 is supplied by an external equipment (compressor), providing the necessary pressure differential for the air to travel through the piping.

Variation of Air Mass Flow Rate -50% Current 50% 100% 150% 200% Mass Flow Rate [kg/s] 0,0036 0,0073 0,0110 0,0220 0,0552 0,1657 Outlet Temperature [°C] 118,07 71,54 56,02 40,51 31,20 27,07 82,49 82,00 81,84 82,34 84,59 Exergy Destruction [%] 81,86

Table 14. Data obtained from adjusting the airflow rate

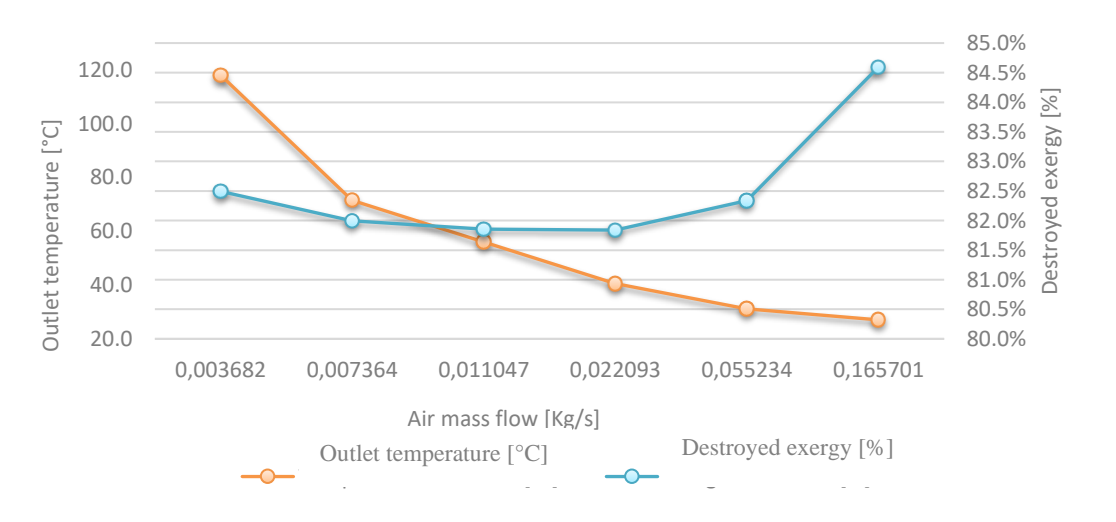


Figure 9. Sensitivity graph case 3

Figure 9 shows that the outlet temperature decreases as the mass flow rate of air increases. The main reason for this behavior is the contact time of the air in the piping, which acts as a heat exchanger; at higher flow rates, the velocity increases, resulting in a less efficient heat transfer process to the air. Regarding exergy destruction, it

should be noted that the energy efficiency of the system and the heating value of the cocoa shell are constant. Consequently, the variation in exergy destruction is minimal, tending to increase when the mass flow rate is decreased or increased. This indicates that if improvements are not made directly to the efficiency of the burner, determined by design parameters, significant enhancements in the energy performance of the equipment will not be achieved.

4. Conclusions

The results of the study on the biomass burner show an energy efficiency of 10.62% and an exergetic efficiency of 9.4%. It can be concluded that the system's performance mainly depends on the design configuration of the burner, which capitalizes on the energetic potential of the biomass, as well as the differences between the inlet and outlet air temperatures in the equipment.

The outlet air temperature obtained from the burner is optimal for the drying process of various fruits. However, another important factor to consider is the mass flow rate of air at the outlet, which is 0.0073 kg/s. This is low for the equipment due to the resistance presented by the heat exchanger piping, primarily due to its length and diameter.

The sensitivity analysis provides the necessary information to understand the system's behavior under different scenarios where the most influential process parameters are adjusted. It was determined that even if the mass flow rate of air is varied using more powerful compressors or the lower heating value is adjusted with other types of biofuels if the inherent efficiency of the heat exchanger is not improved, significant enhancements in maximizing the energetic potential of biomass will not be achieved.

Improper construction of a biomass burner can significantly affect the amount of energy generated from the biomass used, as low energy efficiency limits the production of useful energy. If the design and construction of the burner are not optimal, there can be significant heat losses during combustion, resulting in lower production of usable energy. It is recommended to increase the diameter of the heat exchanger coil and to use a material with a higher heat transfer coefficient to enhance its efficiency. This would allow for an increased air flow rate and the use of biofuels with higher energy content, minimizing the losses currently observed.

Symbols

Q Heat Transfer Rate (W)

A Area (m²)

m Mass Flow Rate (kg/s)

 C_n Specific Heat (J/kg·K)

T Temperature (°C or K)

v Velocity (m/s)

l Length (m)

d Diameter (m)

R Ideal Gas Constant (J/mol·K)

P Pressure (Pa)

h Molar Enthalpy (J/mol)

 \bar{s} Molar Entropy (J/mol·K)

e Exergy Flow (J/kg)

Ė Exergy (W)

h Enthalpy (J/kg)

s Entropy (J/kg·K)

X_i Molar Fraction (-)

Y_i Molar Weight (-)

 \bar{x} Average of Experimental Data (-)

t Time (hour or year)

P Electric Power (kW)

Greek symbols

 α Absorptivity (-)

 τ Emissivity (-)

μ Air Friction Coefficient (-)

 η Efficiency (%)

 ρ Density (kg/m³)

 σ Standard Deviation (-)

 δ Measurement Uncertainty (%)

Declaration of competing interest

The authors declare that they have no known financial or non-financial competing interests in any material discussed in this paper.

Funding information

The project was financed by Sistema General de Regalías SGR, Ministerio de Ciencia Tecnología e Innovación, Colombia.

Author contribution

Nilson Yulian Castillo León: Participated in the selection of the study methodology; Arly Dario Rincon Quintero: Supported the analysis, validation, and verification of information; Aldemar Ahythiamder Mosquera Clavijo: Executed the data collection and conceptualization; Carolina Andrea Suarez López: Established the general aspects of the system; Luis Alonso Betancur Arboleda: Performed the analysis of the thermodynamic properties and sensitivity results; Luis Alfonso Del Portillo Valdés: Supported the development, analysis, and translation of the document. All authors participated in the analysis, writing, calculations, and approval of the final manuscript.

References

- [1] J. G. Borja Fajardo, H. B. Horta Tellez, G. C. Peñaloza Atuesta, A. P. Sandoval Aldana, y J. J. Mendez Arteaga, "Antioxidant activity, total polyphenol content and methylxantine ratio in four materials of Theobroma cacao L. from Tolima, Colombia", *Heliyon*, vol. 8, núm. 5, p. e09402, 2022, doi: https://doi.org/10.1016/j.heliyon.2022.e09402.
- [2] J. Neilson, A. Dwiartama, N. Fold, y D. Permadi, "Resource-based industrial policy in an era of global production networks: Strategic coupling in the Indonesian cocoa sector", *World Dev.*, vol. 135, p. 105045, 2020, doi: https://doi.org/10.1016/j.worlddev.2020.105045.
- [3] S. Zadhossein, Y. Abbaspour-Gilandeh, M. Kaveh, M. Nadimi, y J. Paliwal, "Comparison of the energy and exergy parameters in cantaloupe (Cucurbita maxima) drying using hot air", *Smart Agric. Technol.*, vol. 4, p. 100198, 2023, doi: https://doi.org/10.1016/j.atech.2023.100198.
- [4] C. Parida *et al.*, "Exergy assessment of infrared assisted air impingement dryer using response surface methodology, Back Propagation-Artificial Neural Network, and multi-objective genetic algorithm", *Case Stud. Therm. Eng.*, vol. 53, p. 103936, 2024, doi: https://doi.org/10.1016/j.csite.2023.103936.
- [5] Y. C. Mihret, M. A. Delele, y S. T. Hailemesikel, "Design, development, and testing of rice-husk fueled mixed-flow rice dryer for small-scale rice producer farmers", *Heliyon*, vol. 9, núm. 7, p. e18077, 2023, doi: https://doi.org/10.1016/j.heliyon.2023.e18077.
- [6] C. A. Komolafe, M. A. Waheed, S. I. Kuye, B. A. Adewumi, y A. O. Daniel Adejumo, "Thermodynamic

- analysis of forced convective solar drying of cocoa with black coated sensible thermal storage material", *Case Stud. Therm. Eng.*, vol. 26, p. 101140, 2021, doi: https://doi.org/10.1016/j.csite.2021.101140.
- [7] S. Chokphoemphun, S. Hongkong, y S. Chokphoemphun, "Evaluation of drying behavior and characteristics of potato slices in multi–stage convective cabinet dryer: Application of artificial neural network", *Inf. Process. Agric.*, 2023, doi: https://doi.org/10.1016/j.inpa.2023.06.003.
- [8] S. E. Agarry *et al.*, "Transport phenomena, thermodynamic analyses, and mathematical modeling of okra convective cabinet-tray drying at different drying conditions", *Eng. Appl. Sci. Res.*, vol. 48, núm. 5, pp. 637–656, 2021, doi: 10.14456/easr.2021.65.
- [9] A. M. Nikbakht, A. Motevali, y S. Minaei, "Energy and exergy investigation of microwave assisted thin-layer drying of pomegranate arils using artificial neural networks and response surface methodology", *J. Saudi Soc. Agric. Sci.*, vol. 13, núm. 2, pp. 81–91, 2014, doi: 10.1016/j.jssas.2013.01.005.
- [10] M. Castro, C. Román, M. Echegaray, G. Mazza, y R. Rodriguez, "Exergy Analyses of Onion Drying by Convection: Influence of Dryer Parameters on Performance.", *Entropy (Basel)*., vol. 20, núm. 5, 2018, doi: 10.3390/e20050310.
- [11] D. Yogendrasasidhar y Y. Pydi Setty, "Drying kinetics, exergy and energy analyses of Kodo millet grains and Fenugreek seeds using wall heated fluidized bed dryer", *Energy*, vol. 151, pp. 799–811, 2018, doi: https://doi.org/10.1016/j.energy.2018.03.089.
- [12] Z.-L. Liu *et al.*, "Prediction of energy and exergy of mushroom slices drying in hot air impingement dryer by artificial neural network", *Dry. Technol.*, vol. 38, núm. 15, pp. 1959–1970, nov. 2020, doi: 10.1080/07373937.2019.1607873.
- [13] Y. Abbaspour-Gilandeh, A. Jahanbakhshi, y M. Kaveh, "Prediction kinetic, energy and exergy of quince under hot air dryer using ANNs and ANFIS", *Food Sci. Nutr.*, vol. 8, núm. 1, pp. 594–611, 2020, doi: https://doi.org/10.1002/fsn3.1347.
- [14] M. Syamsiro, H. Saptoadi, B. H. Tambunan, y N. A. Pambudi, "A preliminary study on use of cocoa pod husk as a renewable source of energy in Indonesia", *Energy Sustain. Dev.*, vol. 16, núm. 1, pp. 74–77, 2012, doi: 10.1016/j.esd.2011.10.005.
- [15] N. Khani, M. H. Khoshgoftar Manesh, y V. C. Onishi, "Optimal 6E design of an integrated solar energy-driven polygeneration and CO2 capture system: A machine learning approach", *Therm. Sci. Eng. Prog.*, vol. 38, p. 101669, 2023, doi: https://doi.org/10.1016/j.tsep.2023.101669.
- [16] N. C. Cruz, F. C. Silva, L. A. C. Tarelho, y S. M. Rodrigues, "Critical review of key variables affecting potential recycling applications of ash produced at large-scale biomass combustion plants", *Resour. Conserv. Recycl.*, vol. 150, p. 104427, 2019, doi: https://doi.org/10.1016/j.resconrec.2019.104427.
- [17] M. A. Rahim *et al.*, "Characterization and effect of optimized spray-drying conditions on spray-dried coriander essential oil", *Ind. Crops Prod.*, vol. 209, p. 117976, 2024, doi: https://doi.org/10.1016/j.indcrop.2023.117976.
- [18] J. E. Carranza S., Yamid Alberto; Restrepo V., Alvaro Hernán; Tibaquirá G., "Exergy of compressed air", *Sci. Tech.*, 2004.
- [19] I. W. Árpád, J. T. Kiss, y D. Kocsis, "Role of the volume-specific surface area in heat transfer objects: A critical thinking-based investigation of Newton's law of cooling", *Int. J. Heat Mass Transf.*, vol. 227, p. 125535, 2024, doi: https://doi.org/10.1016/j.ijheatmasstransfer.2024.125535.
- [20] B. Doğan, S. Özer, E. Vural, y A. F. Haciyusufoğlu, "Energy, exergy and sustainability analyses of nanoparticles added to fuels to reduce carbon footprint", *Case Stud. Therm. Eng.*, vol. 56, p. 104252, 2024, doi: https://doi.org/10.1016/j.csite.2024.104252.

- [21] A. Aktaş, M. Koşan, B. Aktekeli, Y. Güven, E. Arslan, y M. Aktaş, "Numerical and experimental investigation of a single-body PVT using a variable air volume control algorithm", *Energy*, vol. 307, p. 132793, 2024, doi: https://doi.org/10.1016/j.energy.2024.132793.
- [22] McGraw-Hill, "Tablas de las propiedades del aire a 1 atm de presión", *Mecánica fluidos Fundam. y Apl.*, 2006.
- [23] M. M. Martínez, Combustión y quemadores, núm. 1. Marcombo, 2005.
- [24] A. Hassan, A. M. Nikbahkt, Z. Welsh, P. Yarlagadda, S. Fawzia, y A. Karim, "Experimental and thermodynamic analysis of solar air dryer equipped with V-groove double pass collector: Technoeconomic and exergetic measures", *Energy Convers. Manag. X*, vol. 16, p. 100296, 2022, doi: https://doi.org/10.1016/j.ecmx.2022.100296.
- [25] A. Alrashidi, A. A. Altohamy, M. A. Abdelrahman, y I. M. M. Elsemary, "Energy and exergy experimental analysis for innovative finned plate solar air heater", *Case Stud. Therm. Eng.*, vol. 59, p. 104570, 2024, doi: https://doi.org/10.1016/j.csite.2024.104570.
- [26] I. H. Bell, J. Wronski, S. Quoilin, y V. Lemort, "Pure and Pseudo-pure Fluid Thermophysical Property Evaluation and the Open-Source Thermophysical Property Library CoolProp", *Ind. Eng. Chem. Res.*, vol. 53, núm. 6, pp. 2498–2508, feb. 2014, doi: 10.1021/ie4033999.
- [27] M. Gao, J. Fan, S. Furbo, y Y. Xiang, "Energy and exergy analysis of a glazed solar preheating collector wall with non-uniform perforated corrugated plate", *Renew. Energy*, vol. 196, pp. 1048–1063, 2022, doi: https://doi.org/10.1016/j.renene.2022.07.026.